



1 **Rain concentration and sheltering effect of solar panels on cultivated plots**

2

3 Yassin Elamri<sup>1,2</sup>, Bruno Cheviron<sup>3</sup>, Annabelle Mange<sup>4</sup>, Cyril Dejean<sup>5</sup>, François Liron<sup>6</sup>, Gilles Belaud<sup>7</sup>

4

5 <sup>1</sup> IRSTEA/UMR G-Eau, 361 rue Jean-François Breton 34136 Montpellier (FRANCE), [yassin.elamri@irstea.fr](mailto:yassin.elamri@irstea.fr)

6 <sup>2</sup> Sun'R sas, 41 quai Fulchiron 69005 Lyon (FRANCE), [yassin.elamri@sunr.fr](mailto:yassin.elamri@sunr.fr)

7 <sup>3</sup> IRSTEA/UMR G-Eau, 361 rue Jean-François Breton 34136 Montpellier (FRANCE), [bruno.cheviron@irstea.fr](mailto:bruno.cheviron@irstea.fr)

8 <sup>4</sup> IRSTEA/UMR G-Eau, 361 rue Jean-François Breton 34136 Montpellier (FRANCE), [annabelle.mange@irstea.fr](mailto:annabelle.mange@irstea.fr)

9 <sup>5</sup> IRSTEA/UMR G-Eau, 361 rue Jean-François Breton 34136 Montpellier (FRANCE), [cyril.dejean@irstea.fr](mailto:cyril.dejean@irstea.fr)

10 <sup>6</sup> IRSTEA/UMR G-Eau, 361 rue Jean-François Breton 34136 Montpellier (FRANCE), [francois.liron@irstea.fr](mailto:francois.liron@irstea.fr)

11 <sup>7</sup> Montpellier SupAgro/UMR G-Eau, 2 place Pierre Viala 34060 Montpellier (FRANCE), [belaud@supagro.inra.fr](mailto:belaud@supagro.inra.fr)

12



13 **Abstract**

14

15 Agrivoltaism is the association of agricultural and photovoltaic energy production on the same land  
16 area, coping with the increasing pressure on land use and water resources while delivering a clean  
17 and renewable energy. However the solar panels located above the cultivated plots also have a  
18 seemingly unexplored yet effect on rain redistribution, sheltering large parts of the plot but  
19 redirecting concentrated fluxes on a few locations. The spatial heterogeneity in water amounts  
20 observed on the ground is high in the general case ; its dynamical patterns are directly attributable to  
21 the mobile panels through their geometrical characteristics (dimensions, height, coverage  
22 percentage) and the strategies selected to rotate them around their support tube. A coefficient of  
23 variation is used to measure this spatial heterogeneity and to compare it with the coefficient of  
24 uniformity that classically describes the efficiency of irrigation systems. A rain redistribution model  
25 (AVrain) was derived from literature elements and theoretical grounds then validated from  
26 experiments in both field and controlled conditions. AVrain simulates the effective rain amounts on  
27 the plot from a few forcing data (rainfall, wind velocity and direction) thus allows real-time strategies  
28 that consist in operating the panels so as to limit rain interception mainly responsible for the spatial  
29 heterogeneities. Such avoidance strategies resulted in a sharp decrease of the coefficient of  
30 variation, e.g. 0.22 against 2.13 for panels held flat during one of the monitored rain events, that is a  
31 fairly good uniformity score for irrigation specialists. Finally, the water amounts predicted by AVrain  
32 were used as inputs to HYDRUS-2D for a brief exploratory study on the impact of the presence of  
33 solar panels on rain redistribution at shallow depths within soils : similar, more diffuse patterns were  
34 simulated and coherent with field measurements.

35

36 **Copyright statement**

37

38 Data collection and model development were performed in the frame of the Sun'Agri2B project that  
39 links the Sun'R SAS society with Irstea, SupAgro Montpellier and other academic or non-academic  
40 partners. The copyright on all experimental and theoretical results presented here is governed by the  
41 consortium agreement of the Sun'Agri2B project.

42



43 **1. Introduction**

44 The current climate change context induced by the production and consumption of highly polluting  
45 fossil energies, responsible for the greenhouse effect, has in turn triggered the development of clean  
46 and renewable energies with special interest for photovoltaic systems (IPCC, 2014). The recent times  
47 have seen a clear increase of land coverage by solar panels disposed on roofs, used for parking  
48 shadehouses or organized in solar farms (IPCC, 2011). In the last years, solar panels were installed  
49 above cultivated plots in France (Marrou, 2012), in Japan (Movellan, 2013), in India (Harinarayana  
50 and Vasavi, 2014), in the USA (Ravi et al., 2014) and in Germany (Osborne, 2016) so as not to create  
51 competition between different land uses (Dinesh and Pearce 2016). These innovative devices termed  
52 "agrivoltaic" by Dupraz et al. (2011) allow maintaining the agricultural yield under certain conditions  
53 (Marrou et al., 2013b; Marrou et al., 2013c), together with water savings (Marrou et al., 2013a)  
54 which results in the expected higher values of the dedicated "land use efficiency" indicator (Marrou  
55 2012)

56

57 Besides blocking and converting a part of the incoming solar radiation, the implementation of solar  
58 panels in natural settings has a series of direct or indirect effects on several terms of the hydrological  
59 budget, in the equipped plots (Cook and McCuen 2013; Barnard et al. 2017). Although far less  
60 studied, these on-site or off-site hydrological consequences should be addressed and modeled for  
61 site preservation purposes in the general case and also because they are very likely to constrain the  
62 optimal irrigation and local site management strategies, on the cultivated plots. For example,  
63 Diermanse (1999) showed that a correct simulation of runoff could often be achieved at the  
64 watershed scale from spatially-averaged rainfall values, although clearly better results may be  
65 expected when explicitly accounting for the subscale spatial patterns of rain distribution (Faurès et  
66 al., 1995; Tang et al., 2007; Emmanuel et al., 2015). At the plot scale, rain interception and  
67 redistribution by the crops (Levia and Germer, 2015; Yuan et al., 2017) is already known to cause  
68 strong spatial heterogeneities (through stemflow, throughfall or improved water storage capabilities)  
69 thus to raise multiple questions on soil microbiology, non-point source pollution and irrigation  
70 piloting (Lamm and Manges, 2000; Martello et al., 2015). The presence of solar panels will provide  
71 similar, additional issues, close to these experienced in agroforestry when the vegetative cover is of  
72 various heights and nature, with a direct impact on the spatiotemporal patterns of rain redistribution  
73 (Jackson, 2000). More into details and more specifically, the interception of rain by the impervious  
74 surface of the solar panels produces an "umbrella effect" that delineates a sheltered area. By  
75 contrast, its contour receives the collected fluxes, whose intensity or amounts may locally exceed  
76 these of the control conditions, depending on the dimensions, height and tilting angle of the panels



77 as well as on wind velocity and direction. Cook and McCuen (2013) stated that one benefit of grass  
78 growing was to damp or suppress any specific effect of solar panels on runoff at the plot scale. This  
79 also constitutes valuable preventive measure against erosion issues arising from concentrated flows  
80 in micro-gullies (Knapen et al., 2007; Gumiere et al., 2009) or attributable to the direct mechanical  
81 effects of droplet impacts, known as splash erosion (Nearing and Bradford, 1985; Josserand and  
82 Zaleski, 2003).

83

84 Agricultural soils should preferentially not be left bare under solar panel structures, because of  
85 increased risks of runoff and erosion but these are only the most severe particular cases among the  
86 diverse rain redistribution effects investigated in the present paper. These are possibly described  
87 from geometrical arguments for an intuitive overview, suggesting three categories of zones on the  
88 ground, in the agrivoltaic plots, (i) the non-impacted zones between panels that receive the same  
89 rain amounts as the control site, (ii) the sheltered zones located right under the panels that receive  
90 far less rainfall than in the control conditions and (iii) the border zones located where panels  
91 discharge the collected rain amounts.

92

93 In most cultivated plots, the spatial heterogeneity of rainfall is weak before that of the other  
94 determinants of the water budget and crop yield, typically the lateral and vertical variations of soil  
95 properties and the non-uniformity of irrigation. Conversely, the presence of solar panels may cause  
96 strong spatial heterogeneities possibly compared to that of the water abduction systems used for  
97 irrigation, whose efficiency is estimated from the values of a coefficient of uniformity (Burt et al.,  
98 1997; Playán and Mateos, 2006; Pereira et al., 2002). This paper therefore aims at characterizing the  
99 effective rain distribution in agrivoltaic plots from the calculation of discharge volumes at the outlet  
100 of the panels, depending on their tilting angle. Moreover, the procedure applies to mobile panels  
101 endowed with one degree of freedom, i.e. able to rotate around their support tube according to  
102 predefined strategies, which defines and introduces "dynamic agrivoltaism". Water redistribution in  
103 soils comes in accordance and is briefly described here for coherence checks, it is not the main scope  
104 of the manuscript though crucial for crop growth and irrigation optimisation.

105

106 Sect. 2 describes the experimentations conducted on the agrivoltaic plot (Sect. 2.1) and in controlled  
107 conditions (Sect. 2.2), also presenting the AVrain model that predicts rain redistribution by the solar  
108 panels (Sect. 2.3). Sect. 3 shows the experimental and modelling results, discussed in Sect. 4. Sect. 5  
109 gathers the conclusions and openings of this work.

110



111 **2. Material and methods**

112 *2.1. Field experiments*

113 **2.1.1. Agrivoltaic plot**

114 The agrivoltaic plot (AV) located on the experimental domain of Lavalette (IRSTEA Montpellier:  
115 43.6466 °N ; 3.8715 °E) covers an area of 490 m<sup>2</sup>, equipped with four rows of quasi-joined agrivoltaic  
116 panels (PV) oriented North-South. The rectangular panels are 2 m long and 1 m wide for a total  
117 surface coverage of 152 m<sup>2</sup>. They are elevated at 5 m and part of a metallic structure supported by  
118 pillars separated by 6.4 m, forming square arrays, so as to allow agricultural engines in the agrivoltaic  
119 plot. This coverage corresponds to a "half-density" in comparison with a classical free-standing plant.  
120 The tilting angle of the PV may vary between -50° and +50° with reference to the flat, horizontal case.  
121 This 1-degree of freedom rotation around the horizontal, transverse axis of the panels is ensured by  
122 jacks. These may be controlled for solar tracking during daytime or to obey other user-defined time-  
123 variable controls. The measurement campaign spreads from October 18<sup>th</sup>, 2015 to October 24<sup>th</sup>, 2016  
124 thus covers a full year. It encompasses 41 monitored rain events, 12 of which recorded with a 1-  
125 minute time step, among which 11 exhibit complete and reliable sets of data linked to the incoming  
126 and redistributed rain amount, and to the tilting angle of the panels.

127

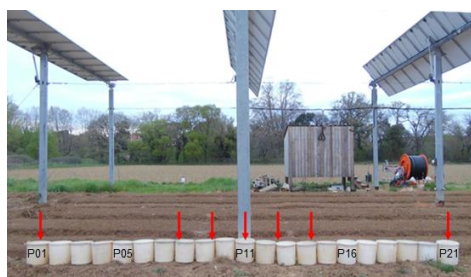
128 **2.1.2. Effective rain and soil water content measurements**

129 The monitoring of rain amounts in the AV plot is ensured by a series of 21 collectors of 0.3 m  
130 diameter, aligned and joined so as to form a continuous line, centered under a PV row, and  
131 transverse to it (Fig. 1). In the following, the collectors are termed P01 to P21 from West to East. In  
132 addition P0 indicates the rain amount collected in control conditions, just beside the AV plot. All rain  
133 amounts collected are expressed as water depths (with 1 mm = 1 L m<sup>-2</sup>). The recordings were made  
134 for various angular positions of the PV, either held flat or in abutment ( $\pm 50^\circ$ ) or during time-variable  
135 "avoidance strategies" that mainly consist in minimizing rain interception by the panels by deciding  
136 their titling angle from wind direction. Rain amounts in the nearby control zone are measured with a  
137 tipping bucket rain gauge (Young 52203, Campbell Sci.). A windvane anemometer (Young 05103-L,  
138 Campbell Sci.) allows recording wind direction and velocity.

139



140 [Fig.1 about here]



141

142

143 **Figure 1 - Effective rain and soil water content measurement under solar panels. Red arrows indicate the position of**  
144 **neutron probes, on a line parallel to that of the collectors, 1 m before it. Some of the P01 to P21 collectors have been**  
145 **identified on the picture for clarity.**

146

147 Soil water content is measured with neutron probes (probe 503DR Hydroprobe, CPN International)  
148 until 1 m depth. The soil is predominantly silty and deep. Seven neutron probes were installed at 0.0,  
149 0.5, 1.0 and 3.2 m on both sides of the axis of rotation of the PV row (Fig. 1). Measurements are  
150 made once or twice a week on a regular basis but systematically before and after the events.

151

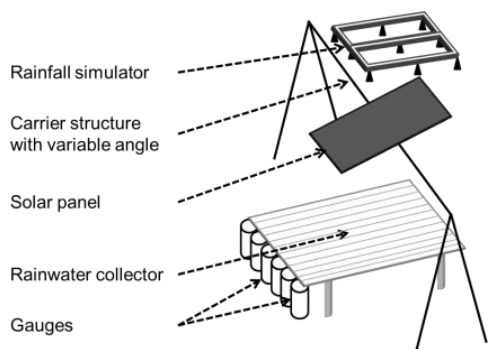
### 152 **2.1.3. Experiments in controlled conditions**

153 A reduced-size agrivoltaic device was built to characterize the influence of the tilting angle of the  
154 panels in indoor conditions, monitoring the collected rain amounts in absence of wind with a focus  
155 on the lateral redistribution on the width of the panels (Fig. 2). The experimental device consisted of  
156 a (2 m x 1 m) panel on a supporting structure of reduced height, allowing tilting angles between 0  
157 and 70°. A rainfall simulator composed of numerous fogging sprays was placed 1.8 m above the flat  
158 position of the panel, ensuring quasi-uniform rain conditions on the whole area of the panel, with  
159 tested intensities of 20, 35, 60 and 70 mm h<sup>-1</sup> selected to be representative of the local rain  
160 intensities. Water flowing out of the panel was collected on a tilted plane on which 10 half cylinders  
161 were fixed, pouring water in the corresponding 10 joined collectors of 0.1 m diameter, covering the  
162 width of the panel. The collected amounts were weighted at the end of each test and converted into  
163 water depths.

164



165 [Fig. 2 about here]



166

167 **Figure 2 - Experimental device used for indoor tests, focusing on lateral rain redistribution on the width of the panel, for**  
168 **various combinations of rain intensities and tilting angles of the panel.**

169

### 170 2.3. Rain redistribution model (AVrain)

#### 171 2.3.1. Model rationale

172 The modelling of rain redistribution by solar panels is a geometrical problem describing rain  
173 interception by an impervious surface of length  $L$ , tilting angle  $\alpha_{pV}$  and height  $h$  above the ground, in  
174 which  $\alpha_R$  is the angle of incidence of rainfall with respect to the vertical axis and  $\theta_R$  denotes the plane  
175 in which the rain falls, with respect to the North in the present case (Fig. 3). The solution is studied in  
176 the vertical  $(x, z)$  plane so that the effects in the  $y$  direction will be discussed and evaluated but not  
177 explicitly described here. Finally,  $E$  is the spacing between the supporting pillars, allowing the  
178 estimation of an equivalent 1-D surface coverage thus the extension of local calculations to the  
179 whole agrivoltaic plot. All notations appear in the Appendix.

180

181

182

183

184

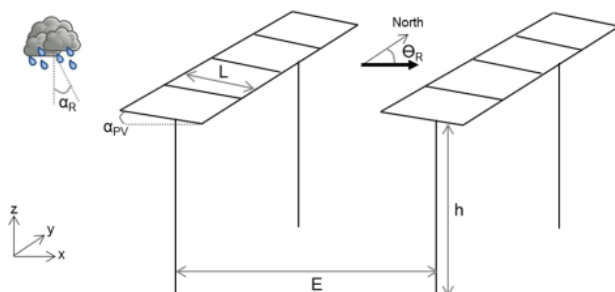
185

186

187



188 [Fig. 3 about here]



189

190

191 **Figure 3 - Scheme of the simulated scene, indicating the key parameters of the AVrain model that describes rain**  
 192 **redistribution by the solar panels on agrivoltaic plots.**

193

194 The angle of incidence of rainfall with respect to  $z$  may be estimated from the ratio between wind  
 195 velocity ( $v_w$ ) and the velocity of the falling rain drops ( $v_d$ ), according to Van Hamme (1992).

$$\tan(\alpha_R) = \frac{v_w}{v_d} \quad (1)$$

196 In the above,  $v_d$  is drawn from the equation proposed by Gunn and Kinzer (1949) for the free-fall limit  
 197 velocity of a rain drop in stagnant air, from measurements obtained with the electrical method,  
 198 relevant for drop diameters ( $D$ ) between 0.1 and 5.7 mm:

$$v_d^2 = \frac{4}{3} \frac{gD(\rho_s - \rho)}{\rho c} \quad (2)$$

199 where  $g$  is the acceleration of gravity,  $\rho_s$  is water density,  $\rho$  is air density and  $c$  is the drag coefficient.

200 Drop size distribution has been linked to rain intensity ( $I$ ) by Best (1950) from previous literature  
 201 elements and measurements made by the author:

$$1 - F_{cum} = \exp\left(-\left(\frac{D}{1.3I^{0.232}}\right)^{2.25}\right) \quad (3)$$

202 where  $F_{cum}$  is the fraction of liquid water in the air comprised in drops with diameters less than  $D$ .

203 The determination of the angle of incidence of rainfall ( $\alpha_R$ ), from given rain intensity ( $I$ ) and wind  
 204 velocity ( $v_w$ ) allows then

205 - to discriminate the zones impacted by the presence of solar panels from these that will receive the  
 206 same rain amounts as in the control zone,





207 - to calculate the water amount intercepted by the solar panels ( $I_{pV}$ ) in function of  $I$ ,  $\alpha_{pV}$ ,  $\alpha_R$ ,  $\theta_{pV}$  and  
208  $\theta_R$ , after Van Hamme (1992):

$$I_{pV} = I (\cos \alpha_{pV} - \tan \alpha_R \sin \alpha_{pV} \cos(\theta_{pV} - \theta_R)) \quad (4)$$

209 For simplicity, it is assumed that no significant lateral redistribution occurs on the width of the  
210 panels, resulting in no variation of the outlet flow in the transverse  $y$  direction. The relevance of this  
211 hypothesis is justified in the following: the tests in indoor conditions were designed to address this  
212 issue. It is also assumed that the wetting phase of the panels before runoff initiation (somehow the  
213 storage capacity of the panels) has no noticeable effects on the calculations. From observations, for  
214 low tilting angles, the  $I_{pV}$  value needed to trigger runoff is 0.2 mm at most which is a weak value  
215 compared to the other values involved in the analysis (and lower than the usual precision of rain  
216 gauges).

217 Runoff velocity ( $V$ ) is calculated with the Manning-Strickler formula, hypothesizing flow width is  
218 much larger than flow depth, which makes flow depth approximately equal to the hydraulic radius.  
219 Manning's  $n$  coefficient is assumed to be  $0.01 \text{ s}^{1/3} \text{ m}^{-1}$  after (Te Chow, 1959) because of the very  
220 smooth glass coating of solar panels.

221 The parabolic trajectory of the drops falling from the panels is calculated in similar ways for any drop  
222 size (i.e., diameter  $D$ ) and characterized by the abscissa at which the free falling drop touches ground  
223 ( $x^*$ ) and the free fall duration ( $t^*$ ):

$$\left\{ \begin{array}{l} x^* = a_x \frac{t^{*2}}{2} + V \cos \alpha_{pV} t^* + x_0 \\ a_x = 2 \cdot 10^{-4} \frac{v_w^2}{D} \\ t^* = \frac{V \sin \alpha_{pV} + \sqrt{(V \sin \alpha_{pV})^2 + 2g z_0}}{g} \end{array} \right. \quad (5)$$

224 where  $a_x$  is the acceleration due to wind in the  $x$  direction,  $V$  is the initial velocity of the fall and  $x_0$  is  
225 the abscissa of the edge of the PV.

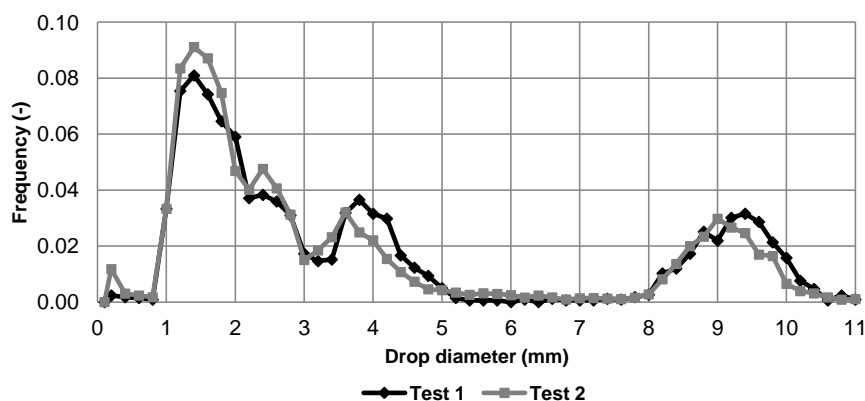
226 Drop diameter measurements in control conditions were conducted with a dual-beam  
227 spectropluviometer (Delahaye et al., 2006) and revealed a three-mode distribution of drop diameters



228 with peaks at  $D=1.4, 3.8$  and  $9.3$  mm (Fig. 4). However, diameters  $D > 7.5$  mm (Niu et al., 2010) might  
229 be artifacts because rain drops this size would become unstable and split in two droplets during their  
230 fall. In the following numerical applications, a fixed diameter of  $D=1.5$  mm is selected as the  
231 reference case for simplicity. However, the sensitivity of the model to  $D$  is weak and will be discussed  
232 later.

233

234 [Fig. 4 about here]



235

236

237 **Figure 4 - Granulometric distribution curve, obtained with a dual-beam spectropuviometer, for the drops falling from the**  
238 **edge of the solar panels. The frequency plotted on the y-axis indicates the count of diameters  $D$  observed with respect to**  
239 **the total count (the step is about 0.2 mm in  $D$ ).**

240

241 The AVrain model was developed with the R software to describe 2D ( $x, z$ ) phenomena in the vertical  
242 plane, hypothesizing negligible effects in the transverse ( $y$ ) direction (Fig. 1). The time step of AVrain  
243 is 1 minute. The required climatic forcings are: rain intensity ( $I$ ), wind velocity ( $v_w$ ) and direction ( $\theta_R$ )  
244 which is assumed identical to rain direction. The input parameters are the geometrical descriptors of  
245 the structure: the height of (the axis of rotation) of the panel ( $h$ ), its length ( $L$ ), tilting angle ( $\alpha_{pv}$ ) and  
246 orientation ( $\theta_{pv}$ ), plus the spacing between (pillars supporting the) solar panels ( $E$ ). Only the tilting  
247 angle can be a function of time as it denotes the control exerted on the system. AV rain allows  
248 calculating rain redistribution (in  $x$ ) in the form of effective cumulative rainfall amounts in function of  
249 time. A known limitation of this simplified model is that the effects of the secondary slopes of the



250 panels are not explicitly accounted for, although properly identified by the experiments in controlled  
251 conditions. These have shown that the combination of low tilting angles (i.e. primary slopes  $\alpha_{pv} < 5^\circ$ )  
252 and low rain intensities lead to lateral homogeneities on the edge of the panels, at the risk of  
253 concentrating water fluxes on the lower corner of the panel in extreme cases. However, the  
254 magnitude of this rain redistribution remains limited in the present experimental and is discussed in  
255 the following.

256

### 257 **2.3.2. Sensitivity analysis**

258 The implementation of solar panels is very likely to affect crop management and irrigation strategies  
259 in the equipped plots, especially because of rain redistribution by the panels. The associated patterns  
260 of spatial heterogeneity may be described by the coefficient of variation (Cv) closely related to the  
261 coefficient that describes the uniformity of water distribution by the irrigation systems (ASAE, 1996;  
262 Burt et al., 1997), thus allowing easy comparisons. The choice of Cv as the target variable for  
263 sensitivity analysis acknowledges spatial heterogeneity is the key descriptor of the effects of solar  
264 panels on rain redistribution on the cultivated plots. In the following, Cv is calculated from the  
265 effective rain amounts (i.e., the cumulative water depths) simulated in the 21 joined collectors along  
266 the x axis. High Cv values indicate strong heterogeneities and Table 1, adapted from ASAE (1996),  
267 recalls the range of Cv values used to qualify the uniformity of water distribution by the irrigation  
268 systems.

269

270

271

272

273

274

275



276 **Table 1 - Reference values for the coefficient of uniformity of water distribution by irrigation systems, after ASAE (1996)**  
277 **and Burt et al. (1997). The original values are expressed here as values of the coefficient of variation used to measure the**  
278 **spatial heterogeneity of rain redistribution by the solar panels.**

279

Performance	Cv
Excellent	< 0.1
Good	0.1-0.2
Fair	0.2-0.3
Poor	0.3-0.4
Unacceptable	> 0.4

280

281

282 Using Cv as an indicator allows accounting for two sources of spatial heterogeneity: rain  
283 redistribution by the solar panels (with eventual local effective rain amounts that exceed the  
284 "natural" rain amounts measured in the control zone) and the sheltering effect of solar panels (with  
285 effective rain amounts far lower right under the panels than in the control zone). More into details,  
286 Cv encompasses in a single indicator the spatial heterogeneity observed within the region located  
287 right under a solar panel, i.e. centered on the transverse y axis that connects two supporting pillars,  
288 as clearly seen in Fig. 1 where the P11 is the central collector. The width of the equipped region is E,  
289 selected as the parameter that describes the spacing between panels and further used to estimate  
290 the 1-D spatial coverage of the plot by the panels, also taking place in the sensitivity analysis of the  
291 model.

292

293 The Morris (1991) method is used with Cv as the target variable, to estimate the sensitivity of the  
294 AVrain model to assess the effect of its seven main parameters (see Table 2) on the spatial  
295 heterogeneity of rain redistribution by the solar panels. The combined "one-at-a-time" screenings of  
296 the parameter space introduced by Campolongo et al. (2007) have been used to cover a wide set of  
297 possible agrivoltaic installations, keeping all parameters within acceptable, realistic ranges of values.  
298 The "sensitivity" package of R (Pujol et al., 2017) was used to generate the associated 4000  
299 parameter sets, obtained from p=7 parameters with d=500 draws each, dispatched within r=8 levels.



300 The control parameter (tilting angle  $\theta_{PV}$  of the panels) was taken between  $-70^\circ$  and  $+70^\circ$  but held  
301 fixed for the tested event ( $P=3.6$  mm,  $v_w=0.78$  m s $^{-1}$ ,  $\theta_w=285^\circ$ , described later).

302

303 **Table 2 - Parameters and ranges of values used in the sensitivity analysis of the AVrain model**

Parameter	Description	Reference	Range	Unit
D	Size of the drops falling from the solar panels	1.5	0.1 - 7	mm
E	Spacing between solar panels	6.40	4 - 10	m
FactorP	Multiplying factor for precipitations	1	0.1 - 10	-
FactorV	Multiplying factor for wind velocity	1	0.1 - 10	-
H	Height of the solar panels	5.00	3 - 7	m
L	Lenght of the solar panels	2.00	1 - 3	m
$\theta_{PV}$	Tilting angle of the solar panels	0	-70 - 70	$^\circ$

304

305

#### 306 *2.4. Control simulations of soil moisture field by Hydrus-2D*

307

308 Hydrus-2D (Simunek et al., 1999) may be used to simulate water redistribution in soils for different  
309 fixed tilting angles of the solar panel or strategies in operating the panels. The simulation domain  
310 finds itself in a vertical (x, z) plane, it is centered on the supporting pillar of a panel and covers a total  
311 width of 6.4 m, corresponding to the distance between two consecutive pillars. Hydrus-2D is rather  
312 used here for coherence checks and to gain an overview of water redistribution in soil than for  
313 detailed numerical simulations of the wetting front movements in space and time, thus allowing  
314 simplifying hypotheses on soil structure. The investigated soil depth is 1-m deep, well-known from  
315 numerous local experiment and predominantly silty. It is assumed homogeneous in absence of  
316 significant contrast with depth and presented in Table 3.

317

318

319



320 **Table 3 - Soil parameters at the Lavalette experimental station used in Hydrus-2D, after Barakat et al. (2017, submitted).**  
 321  $\theta_r$  and  $\theta_s$  denote respectively the residual and saturated volumetric soil water contents,  $\alpha$  and  $n$  are empirical shape  
 322 parameters of Van Genuchten-Mualem model,  $K_s$  is the soil hydraulic conductivity at saturation and  $l$  is a pore  
 323 connectivity parameter.

324

Depth (cm)	Clay (%)	Silt (%)	Sand (%)	$\theta_r$ (-)	$\theta_s$ (-)	$\alpha$ ( $\text{cm}^{-1}$ )	$n$ (-)	$K_s$ ( $\text{cm hr}^{-1}$ )	$l$ (-)
0 – 100	18	42	40	0.01	0.36	0.013	1.2	2.30	0.5

325

326

327 The AVrain model provides the time-variable forcing data at the soil-atmosphere interface for  
 328 Hydrus-2D, divided into five categories and accounting for time-variable tilting angles of the solar  
 329 panel (Fig. 5):

- 330 - atmospheric conditions for zones not impacted by the presence of the solar panel,
- 331 - flux 1 (F1) conditions for zones impacted by the panel and located right under it,
- 332 - flux 2 (F2) conditions for zones impacted by the panel but not located under it,
- 333 - flux 3 (F3) conditions for zones located under the edge of the panel thus exposed to the largest  
 334 effective rain amounts,
- 335 - flux 4 (F4) conditions for zones adjacent to these of the F3 conditions but on the sheltered side.

336

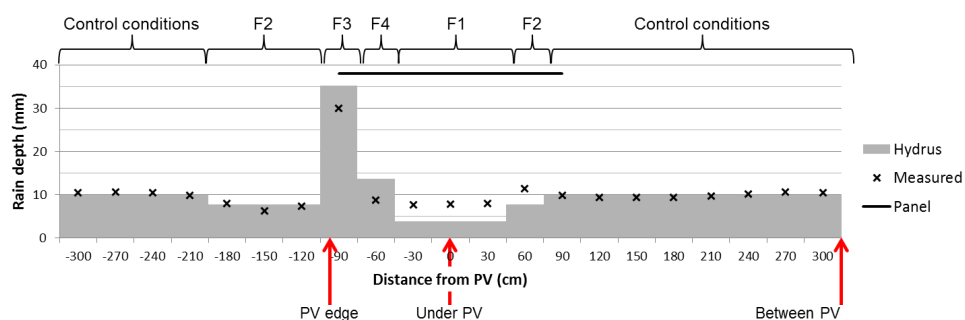
337 Hydrus-2D currently allows five types of time-variable upper boundary conditions, which suggests  
 338 using F2 on both sides of the panel, as indicated in Fig. 5 where only the leftmost position of F2  
 339 corresponds to the choices listed above. However, the rightmost position of F2 seems the most  
 340 suitable default choice given the known soil filling dynamics and the expected effective rain amounts.  
 341 Zero-flux boundary conditions apply on the vertical limits of the domain and free drainage is relevant  
 342 for a bottom boundary condition because the water table is several meters under the limit of the  
 343 domain. For simplicity, the initial soil water content will be assumed homogeneous, selecting a value  
 344 close to the available observations ( $\theta=0.15$ ).

345

346



347 [Figure 5 about here]



348

349 **Figure 5 - Time-variable upper boundary conditions used in Hydrus-2D for the tested rain event, during which the tilting**  
 350 **angle of the panels was varied to minimize rain interception (avoidance strategy).**

351

### 352 3. Results

#### 353 3.1. Rain redistribution measurements on the dynamic agrivoltaic plot

354

355 The influence of variable-tilting angle solar panels on rain redistribution was measured for a wide  
 356 series of rain events covering a full year, taking the coefficient of variation ( $C_v$ ) as the target variable  
 357 thus assuming this measure of spatial heterogeneity is the crucial hydrological descriptor in  
 358 agrivoltaic contexts. Table 4 gathers  $C_v$  values obtained for the most documented rain events in the  
 359 available records. It enables comparisons between  $C_v$  and the tilting angle (or operating strategy) of  
 360 the solar panels, for various rain intensities. The least heterogeneous rain redistributions were  
 361 observed for panels in abutment (Fig. 6a, b) mainly due to decreased surface coverage, from 30% for  
 362 flat panels to 20% for panels in abutment, resulting in a lesser rain interception. However, the  
 363 relevancy of this strategy depends on the angle of the wind with respect to the panels ( $\alpha_R$  vs.  $\theta_R$ )  
 364 identifying these as second-order but non-negligible factors, according to which  $C_v$  may become  
 365 twice as large for panels "facing the wind" or "back to the wind". By contrast, the most  
 366 heterogeneous rain redistribution was observed for a flat panel ( $\alpha_{PV}=0$ ) maximizing rain interception  
 367 and concentration by the panel (Fig. 6c), collecting 11 times more rain than in the control zone, in the  
 368 F4 domain of Fig. 5, with  $C_v=2.13$ .

369



370 Strategies involving time-variable tilting angles  $\alpha_{PV}$  offer multiple possibilities, among which the  
 371 previously mentioned "avoidance strategy" is relevant to decrease the spatial heterogeneity (Fig. 6d)  
 372 and results in  $Cv=0.22$ , that is a fairly good homogeneity according to Table 1. For all the events listed  
 373 in Table 4, only the avoidance strategy was able to provide an acceptable level of uniformity in the  
 374 agrivoltaic plot, i.e. a spatial heterogeneity than would not need to be corrected on purpose, with a  
 375 dedicated precision irrigation device, to ensure equivalent water availability conditions during crop  
 376 growth. In all cases, the effective rain depth was more important on the sides of the panel (collectors  
 377 9 and 13 in Fig. 1 and Fig. 6). There are non-impacted zones in the free space between panels, where  
 378 the effective rain is the same as in the control zone. On the contrary, the sheltering effect is strong  
 379 right under the panels and the effective rain is always far lower than in natural conditions.

380

381 **Table 4 - Rain events with their identification (ID), date, rain amounts on the control zone (P0), tilting angle of the solar**  
 382 **panels ( $\alpha_{PV}$ ) and the associated measured coefficient of variation (Cv) whose highest values indicate the strongest spatial**  
 383 **heterogeneities in rain redistribution by the solar panels. In the comments Sect., "avoidance strategy" indicates a time-**  
 384 **variable  $\alpha_{PV}$  angle to minimize rain interception by the panels in real time.**

385

ID	Date	P0 (mm)	$\alpha_{PV}$	Cv (-)	Comments
#01	18/10/2015	4.8	-50 to 0°	1.14	Solar tracking
#02	07/12/2015	5.1	-50 à -30°	0.98	Solar tracking
#03	12/02/2016	14.6	-50°	0.97	Transverse wind (south)
#04	09/03/2016	5.1	-50°	0.96	Facing the wind
#05	17/03/2016	4.1	+50°	0.40	Back to the wind
#06	21/04/2016	3.6	0°	2.13	Flat panel
#07	30/04/2016	3.0	0°	1.15	Flat panel
#08	22/05/2016	8.4	0°	0.72	Flat panel
#09	28/05/2016	13.5	0°	1.28	Flat panel
#10	31/05/2016	4.5	0°	1.63	Flat panel
#11	14/09/2016	14.8	-50 to +50°	0.22	Avoidance strategy
#12	12/10/2016	203.6	0 °	0.51	Flat panel

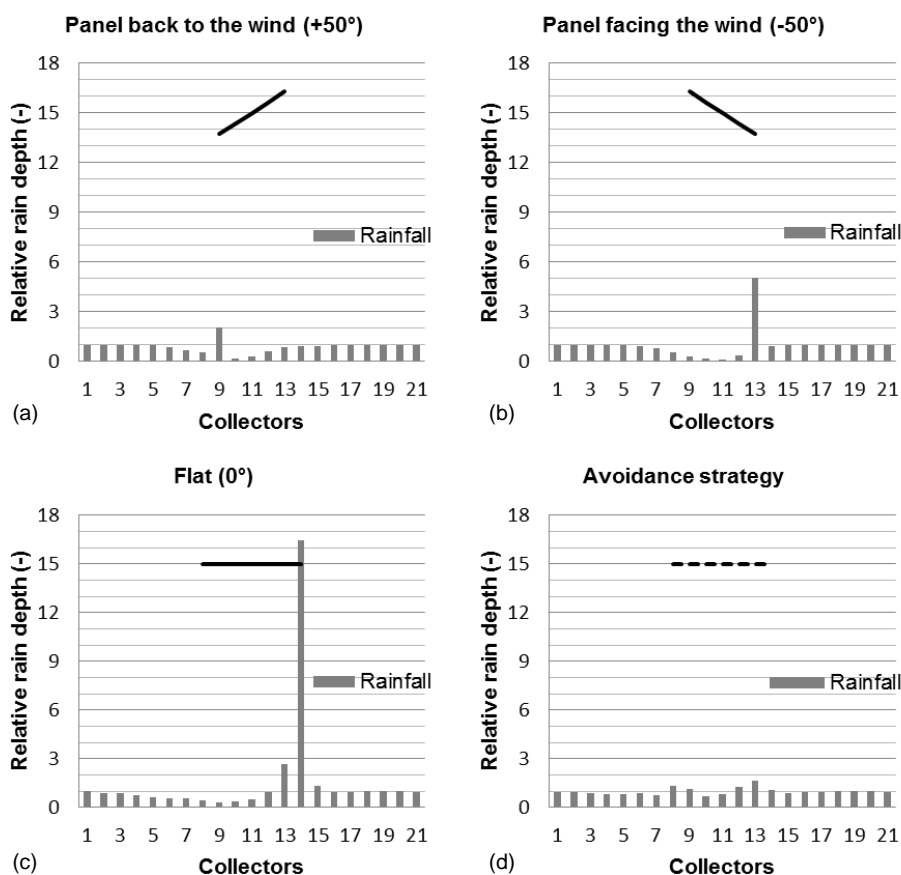
386

387





388 [Figure 6 about here]



389

390 **Figure 6 - Examples of rain redistribution for various rain events, tilting angle and operating strategies of the solar panels,**  
 391 **measured in the collectors displayed in Fig. 1. Relative rain depths are given with respect to the control zone where rain**  
 392 **amounts are collected in the pluviometer.**

393

### 394 3.2. Evaluation and sensitivity analysis of the AVrain model

395

396 The rain redistribution model AVrain was tested for 11 rain events involving flat panels, panels in  
 397 abutment (either back to the wind or facing the wind) and avoidance strategies, as presented in  
 398 Table 5. AVrain describes rain redistribution with a satisfying mean determination coefficient of  
 399  $R^2=0.88$ . The values of MAPE (Mean Absolute Prediction Error) mostly comprised between 0.1 and



400 0.3 and regression coefficients greater than 1 indicate that the model tends to overestimate the real  
 401 effective rain amounts. However, Fig. 7 shows that the overestimations occur near the drip line (i.e.,  
 402 the aplomb) of the panels, totalizing about 25% of the committed errors.

403

404 **Table 5 - Performances of the AVrain model that describes rain redistribution by the solar panels, identifying each event**  
 405 **(ID), indicating the Mean Absolute Prediction Error (MAPE), Normalized Root Mean Square Error (NRMSE), linear**  
 406 **correlation coefficient and coefficient of determination ( $R^2$ ) next to the simulated coefficients of variation (Cv). The**  
 407 **highest Cv values signal the strongest spatial heterogeneities in rain redistribution by the solar panels.**

408

ID	MAPE	NRMSE	Linear correlation coefficient	$R^2$	Cv
#01	0.29	0.22	1.21	0.89	1.15
#02	0.25	0.22	1.45	0.86	1.21
#03	0.41	0.10	0.82	0.83	0.75
#05	0.07	0.13	1.10	0.86	0.46
#06	0.14	0.13	1.06	1.00	2.28
#07	0.21	0.20	0.89	0.98	1.25
#08	0.13	0.11	0.88	0.99	0.72
#09	0.23	0.12	1.38	0.97	1.50
#10	0.22	0.17	1.04	0.96	2.34
#11	0.11	0.08	1.00	0.75	0.19
#12	0.17	0.03	1.13	0.56	0.78

409

410

411

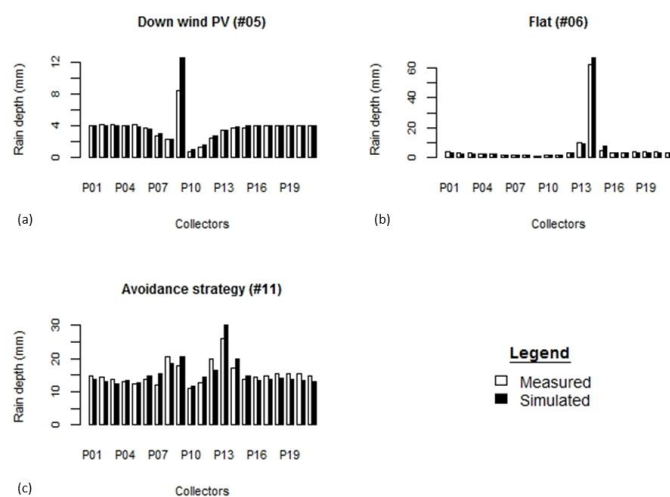
412

413

414



415 [Figure 7 about here]



416

417 **Figure 7 - Examples of rain redistribution by the solar panels simulated by the AVrain model and compared to field**  
418 **measurements, for three very different events and managements of the solar panels (see Tables 4 and 5 for details).**

419

420 The sensitivity analysis of AVrain was conducted with the Morris (1991) method, modified and  
421 improved by Campolong et al. (2007), selecting  $C_v$  as the target variable. Figure 8 shows its results,  
422 where  $\mu^*$  on the x-axis is the mean of the individual elementary effects (thus the sensitivity of the  
423 parameter tested alone) and  $\sigma$  on the y-axis represents the standard deviation of the elementary  
424 effects (thus the sensitivity of the parameter tested in interaction with other parameters). The Morris  
425 plot allows identifying the parameters that have i) a negligible overall effect, denoted by low values  
426 of both  $\mu^*$  and  $\sigma$ , ii) a linear effect, denoted by high values of  $\mu^*$ , or iii) non-linear or interactive  
427 effects, denoted by high values of  $\sigma$ . The sensitivity measures ( $\mu^*$ ,  $\sigma$ ) reported in Fig. 8 for each  
428 parameters have been normalized by the value of the highest sensitivity measure ( $\sigma$ ) for the most  
429 sensitive parameter (FV).

430

431

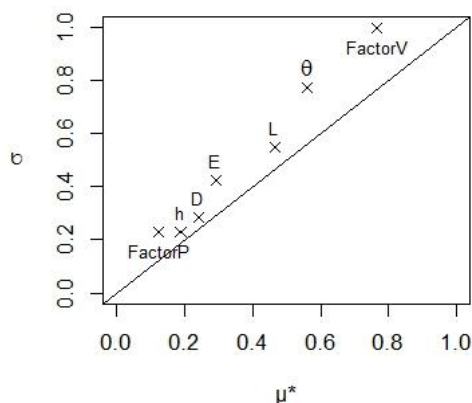
432

433

434



435 [Figure 8 about here]



436

437 **Figure 8 - Sensitivity analysis of the AVrain model by the Morris (1991) method improved by Campolongo et al. (2007),**  
438 **where  $\mu^*$  indicates the linear part of the total sensitivity score for each parameter while  $\sigma$  indicates the non-linear or**  
439 **interactive part. In the Morris plot, D is the drop diameter, E the spacing between solar panels, FP the multiplying factor**  
440 **for precipitations with respect to the reference case, FV the multiplying factor for wind velocity with respect to the**  
441 **reference case, h the height of the solar panels, L their length and  $\theta_{pv}$  their tilting angle (see Table 2 for the reference**  
442 **values and ranges of the parameters). The target variable of the analysis was the coefficient of variation that measures**  
443 **the spatial heterogeneity of rain redistribution by the solar panels. The tested rain event was #06 in Tables 4 and 5.**

444

445

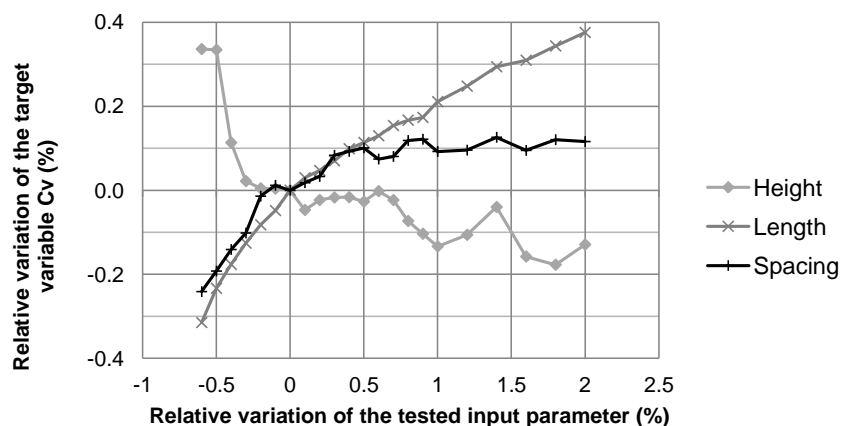
446 The position of the parameters above the 1:1 line in Fig. 8 signals that AVrain is more sensitive to the  
447 interactions between parameters than to individual variations of the parameter values which  
448 reinforces the fact that strong heterogeneities in effective rain amounts most likely occur when  
449 several conditions are met at once, in the forcings (wind direction, drop size), the controls (tilting  
450 angle) and the structure (fixed characteristics of the panels). In particular, the high sensitivity score of  
451 FV compared to the low score of FP indicates that wind velocity tends to influence rain redistribution  
452 patterns far more than rain amounts, likely because wind velocity intervenes in the calculation of the  
453 angle of incidence of rainfall and in that of the trajectory of the drops falling from the panels. The  
454 drop size itself was found of non-negligible but of rather weak influence, although a wide range (0.1  
455 to 7.0 mm) of values was tested. The fact that AVrain is more sensitive to the tilting angle (control  
456 exerted on the system) than to the structure parameters (fixed once selected during the installation)



457 is a crucial result of the analysis, indicating there is room for optimisation. Conversely, the higher  
458 sensitivity of AVrain to wind velocity than to the tilting angle confirms that the optimisation  
459 strategies should be decided from wind characteristics that dictate the angle of incidence of rainfall.  
460 In an overview of Fig. 8, the Morris method unveils the hierarchy of effects. This proves especially  
461 useful when investigating the interactions between the structure parameters. For example, the  
462 combinations between panels length and spacing (defining surface coverage) are expected to have  
463 more effect on the target variable than the combinations involving panel height, making height a  
464 second-order parameter, at least for the tested (realistic) ranges of values and the chosen target  
465 variable. This conclusion would have been impossible to reach when separately testing the effects of  
466 variations in length, spacing and height of the panels, as proven by Fig. 9 which only acknowledges  
467 adverse effects (on Cv) of length and spacing on the one side, and of height on the other side.

468

469 [Figure 9 about here]



470

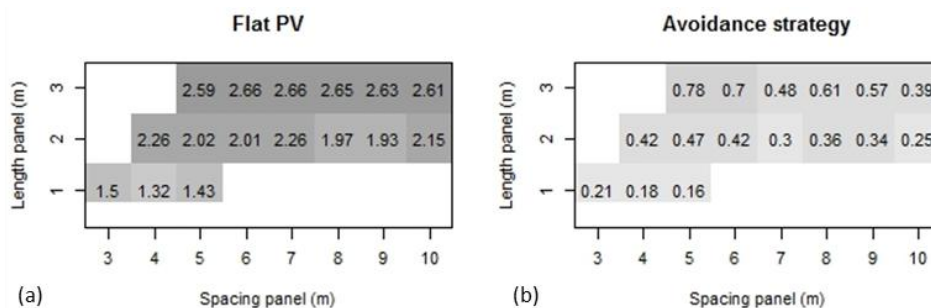
471 **Figure 9 - Spider diagram showing the influence of the structure parameters (spacing E, height h, length L) of the**  
472 **agrivoltaic installation on the spatial heterogeneity of rain redistribution by the solar panels, from the simulated values**  
473 **of the coefficient of variation (Cv).**

474

475 From Fig. 8, the influence of the tilting angle may be expected larger than that of the structure  
476 parameters, anticipating thus that the avoidance strategy (i.e., operating the panels so as to  
477 minimize rain interception) will be prone to significantly reduce Cv whatever the structure



478 parameters. This point is further investigated by Fig. 10, comparing a flat panel with a piloting of the  
 479 panel according to the avoidance strategy, for various combinations of panels length and spacing  
 480 (previously proven to have more influence on Cv than the height of the panels). Small-sized panels  
 481 with a weak spacing between them is advocated as the best configuration to reduce Cv in avoidance  
 482 strategies, simulated to be far more efficient than panel held flat. However, this analysis indicates the  
 483 direction to follow when only rain redistribution issues are tackled but external constraints will surely  
 484 exist when deciding the in-situ implementation of such agrivoltaic installations, for example in the  
 485 form of limit values for the spacing between panels (to allow agricultural activities).  
 486  
 487 [Figure 10 about here]



488 (a) (b)  
 489 **Figure 10 - Influence of the structure parameters (spacing E, length L) of the panels on the spatial heterogeneity of rain**  
 490 **redistribution, from the simulated values of the coefficient of variation (Cv) for panels held flat (a) or operated according**  
 491 **to the avoidance strategy (b). The combinations of E and L values may be assimilated to equivalent 1-D surface coverage**  
 492 **between 20 and 60% by dividing L by E. Only the realistic combinations have been simulated here: blank cells indicate**  
 493 **those that are not.**

494

### 495 3.3. Rain redistribution in soils

496

497 Water content profiles were measured in the agrivoltaic plot immediately before one of the rain  
 498 events, then 6 to 12 hours after it, to identify the dynamics and magnitude of rain redistribution in  
 499 soils, as a consequence of rain redistribution on the soil surface. As expected, the spatial  
 500 heterogeneity observed on the soil surface is transferred but becomes a bit fuzzy in the first 30 cm of  
 501 soil, due to "lateral homogenization" (ponding with significant surface runoff, lateral diffusion



502 associated with soil dispersivity). But still the spatial patterns are clearly visible within soils, especially  
503 for the flat panels case (Fig. 11a) for which three distinct zones may be identified, i) between panels,  
504 with similar behavior as in the control zone, ii) under panels, with a noticeable sheltering effect thus  
505 drier soils and iii) under the edge of the panels, where the increased soil water content is attributable  
506 to the large effective amounts poured on the soil surface. In Fig. 11a, The maximal soil water storage  
507 variation as observed under the edge of the panels, estimated at 6.7 mm in accordance with the  
508 location of the effective rain amount poured on the soil surface (24.0 mm). Between panels, the  
509 storage variation was 2.0 mm for 3.0 mm of effective rain. Under panels, the storage variation was  
510 4.7 mm for only 1.3 mm of effective rain, which reinforces the hypothesis of lateral redistribution,  
511 either within the soil or at its surface, from the nearby zones. In Fig. 11b, the avoidance strategy  
512 tested for a rain event of 60 mm in the control zone resulted in a maximal storage variation of 91 mm  
513 between panels due to a dryer initial soil water content, 76 mm under panels and 43 mm near the  
514 aplomb of the edge of the panels, while significant ponding was observed.

515

516

517

518

519

520

521

522

523

524

525

526

527

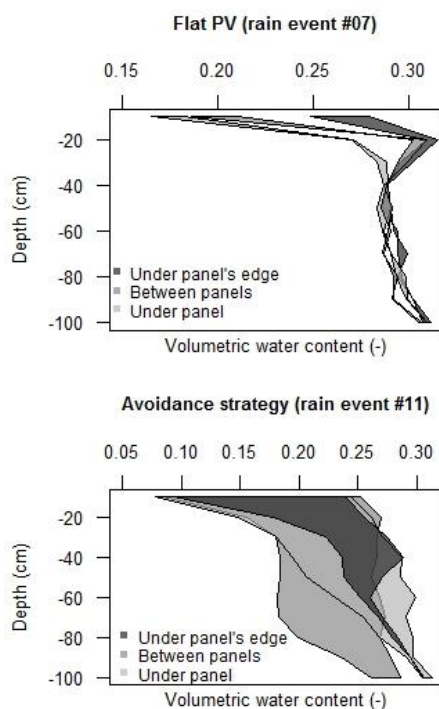
528

529

530



531 [Figure 11 about here]



532

533 **Figure 11 - Variations of soil water storage in soil regions located near the aplomb of panels edge (dark grey), between**  
534 **panels (medium grey) and under panels (light grey) for different strategies in operating the panels, holding panels flat**  
535 **during rain event #07 (a) or operating them according to the avoidance strategy that minimizes rain interception, during**  
536 **rain event #11 (b). For each case, the leftmost and rightmost line indicate the water content profile before and after the**  
537 **event, respectively. Event #11 was considered as the sum of two successive events for a total rainfall of 60 mm in the**  
538 **control zone.**

539

540 The simulation of rain redistribution in soils was made by Hydrus-2D for a single rain event (#11) to  
541 compare the soil water content fields obtained in the flat panel case (Fig. 12a) or when using the  
542 avoidance strategy (Fig. 12b). The time-variable atmospheric conditions required by Hydrus-2D were  
543 provided by the outputs of AVrain at the minute time step, with the five-zone discretization  
544 discussed in Sect. 2.4 and shown in Fig. 5. Starting from a rather dry, realistic and approximately  
545 homogeneous soil water content of  $\theta=0.15$ , the objective of these exploratory simulations were not  
546 to capture the finest spatial patterns of the wetting front; it was rather to assess if the observed

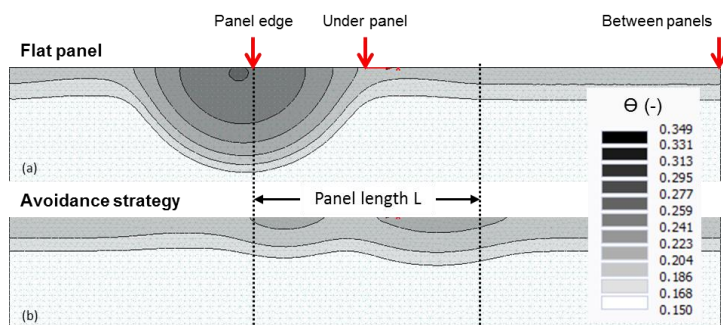




547 noticeable differences in rain redistribution trends could easily be reproduced and quantified by  
548 Hydrus-2D. As expected, the flat panel case leads to the creation of a sharp contrast of soil water  
549 content, near the aplomb of the edge of the panel, in the form of a wet bulb that propagates  
550 downward by gravity and sideward by diffusion. This result in the vertical plane is in coherence with a  
551 well-known 3D effect of irrigation, that the vertical and horizontal deformations of the ellipsoidal  
552 bulb will depend on soil properties: coarse soils will produce very elongated bulbs in the vertical  
553 direction while silty soils are likely to produce more significant lateral redistribution. However, the  
554 simulated spatial heterogeneities in soil water content remain very pronounced for the flat panel  
555 case in comparison with the avoidance strategy (Fig. 12b). In this manuscript, the choice of the  
556 coefficient of variation (Cv) to qualify the spatial heterogeneities allowed the reconnection to the  
557 coefficient of uniformity classically used in irrigation science, addressing water delivery on the soil  
558 surface, typically by sprinkler irrigation. Here, Fig. 12a resembles the 2D or 3D patterns characteristic  
559 of surface or subsurface drip irrigation while Fig.12b recalls the quasi-1D patterns of (high-  
560 performance) sprinkler irrigation.

561

562 [Figure 12 about here]



563

564

565 **Figure 12 - Simulation of soil water patterns with Hydrus-2D, in regions located near the aplomb of panels edge, under**  
566 **panels or between panels, when holding the panels flat (a) or operating them according to the avoidance strategy (b) to**  
567 **reduce the heterogeneity of rain redistribution by the panels, during Event #11 (see Tables 4 and 5). The vertical arrows**  
568 **recall the positions of the neutron probes used to collect water content data plotted in Fig. 11.**

569

570



571 *3.4. Effects of the transverse slope of the panels*

572

573 The underlying hypotheses made in the construction of the AVrain model led to the formulation of a  
574 2D (x, z) model, discarding thus all phenomena arising from variations in the transverse (y) direction  
575 or, at least, not representing them in explicit manner. If relevant, indirect assessments of their effects  
576 should still be made, outside AVrain but to investigate if the model stays valid -or in which conditions  
577 significant uncertainties may exist on its predictions. Among transverse effects likely to exist in real  
578 conditions, only the effects of transverse slopes of the panels were anticipated, observed and  
579 deemed significant, though limited to particular contexts. These contexts are summed up in the cases  
580 when the tilting angle (i.e. the prevalent slope) of the panels is very low, so that the transverse,  
581 secondary slope becomes of the same order.

582

583 Tests in controlled conditions were conducted during 15 minutes, under a rain intensity of  $20 \text{ mm h}^{-1}$ .  
584 Rain redistribution on the width of the panel appears for tilting angles lower than  $20^\circ$  and the width  
585 of the outlet becomes very narrow for tilting angles lower than  $5^\circ$  (Fig. 13). In the latter case, about  
586 90% of the collected water drops from the panel through a 20-cm wide outlet. In the general case,  
587 such effects may be explicitly calculated from the slopes (prevalent, secondary) and water depth on  
588 the panel. Such effects are prone to increase the effective rain amounts observed in the field, at the  
589 aplomb of the edge of the flat panels (Fig. 6c).

590

591

592

593

594

595

596

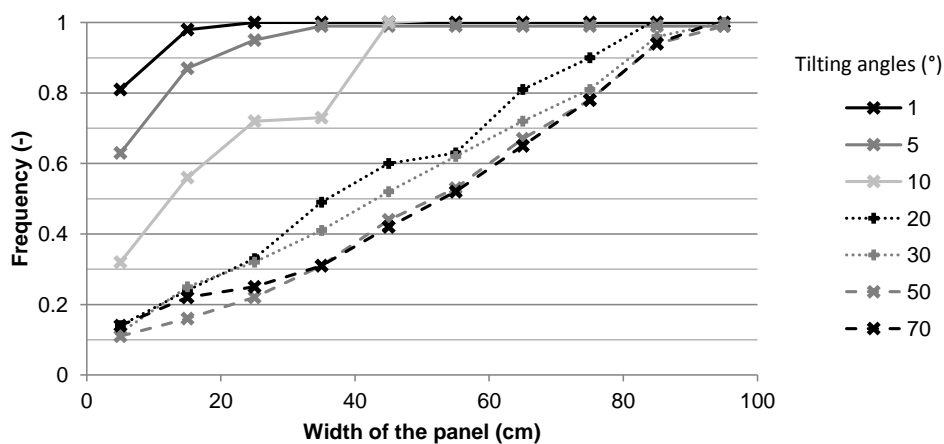
597

598

599



600 [Figure 13 about here]



601

602 Figure 13 - Influence of the transverse slope of the solar panels on the lateral rain redistribution on the width of the  
603 panel, tested for a 20 mm h<sup>-1</sup> rain intensity and "prevalent" tilting angles of the panels between 1 and 70°. The results  
604 are expressed in cumulative distribution of the collected amounts, at the outlets placed along the width of the panel.

605

#### 606 4. Discussion

##### 607 4.1. Rain redistribution by the solar panels

608

609 The 2D AVrain model was developed to describe rain interception and redistribution by the solar  
610 panels and fulfills its objectives well: it allows the identification of the sheltered zones and of the  
611 zones in which the effective rain amounts exceed the natural rain amounts of the control zone, with  
612 a correct quantification of the associated fluxes. The angle of incidence of rainfall was found a key  
613 variable in the determination of the spatial patterns of heterogeneity in the effective rain amounts  
614 falling on the ground. This angle is difficult to measure but the equations derived by Gunn and Kinzer  
615 (1949) and Best (1950) allow to estimate it in indirect ways.

616

617 If relevant, the AVrain model may be adapted to account for additional geometrical characteristics of  
618 the solar panels, for example to better describe the effects of the secondary (transverse) slope when  
619 it becomes of the same order as the tilting angle of the panels (i.e. their prevalent slope). This is the  
620 typical case in which the secondary slope is prone to increase the heterogeneity of rain redistribution



621 by redistributing the collected water along the width of the panels. The presence and effect of a  
622 ridge on the length and/or width of the panels could be explicitly modeled with the techniques used  
623 in hydrology for thin flows over a weir. Even if the presence of a small ridge may affect the threshold  
624 of (approximately) 2 mm water depth thought to trigger runoff on the panels (in controlled  
625 conditions and without a ridge), it is hypothesized here that any explicit modelling would not provide  
626 a significant added value, for two reasons: the stored volumetric amounts are weak when the panels  
627 are held nearly flat in absence of rain and the avoidance strategy is recommended when rain occurs.

628

#### 629 *4.2. Rain redistribution in soils*

630

631 Hydrus-2D was used to simulate rain redistribution in soils, using the spatially distributed output  
632 variables of the AVrain model to provide the required time-variable atmospheric conditions. Five  
633 such conditions at most can be used as climatic forcings for Hydrus-2D, which seemed a limitation for  
634 the present purpose but could be handled, thus with the a posteriori indication that the chosen  
635 "trick" has the value of a good practice. In coherence with the field observations, the simulated fields  
636 of soil water content emphasized the interest of using the avoidance strategy to decrease the spatial  
637 heterogeneities of soil water content in the agrivoltaic plots, confirming thus that the tilting angle of  
638 the panels is a strong control parameter.

639

640 Even if the spatial heterogeneity of rain redistribution is less drastic in soils than on the soil surface,  
641 due to lateral diffusion, it remains strong enough to necessitate a dedicated remediation in the form  
642 of precision irrigation, unless the avoidance strategy is used. In other words the avoidance strategy  
643 (that consists in minimizing rain interception and redistribution by commanding the appropriate  
644 time-variable tilting angle of the panels) has implications in the relevant irrigation strategy, making it  
645 less complex. This is an opening to a more global optimisation problem in dealing with the various  
646 sources of heterogeneity, certainly to be compared with the observed heterogeneities in crop yield  
647 on the agrivoltaic plots. Besides the heterogeneities in the forcings (irrigation and rain redistribution)  
648 the modeller will surely have to also address these in soils, for example by means of geophysical



649 methods that offer the possibility of similar spatial resolutions (e.g., electrical resistivity tomography,  
650 refraction seismology)

651

#### 652 *4.3. Rain and crop-induced operation of solar panels*

653

654 Some aspects specific to cultivated plots need to be mentioned here, although the primary scope of  
655 this paper is to focus on the hydrological side. The panels left with a low tilting angle (high surface  
656 coverage and rain interception) are prone to have unwanted direct effects on the soil and plants  
657 underneath. For example, leafy vegetables might be damaged by the repeated drop impacts or even  
658 more by the occasional curtains of water falling from the panels a few meters above, even if their  
659 storage capacity is limited. Such problems will typically occur in the morning, when panels are first  
660 operated, being that they are generally left flat during nighttime. They could also occur during heavy  
661 rains, even when using the avoidance strategy, which results in a damped but non-zero flux  
662 concentration near the aplomb of the edges of the solar panels. In the bare soil periods, it is rather  
663 the erosion risk that should be handled, especially "splash erosion" (Nearing and Bradford, 1985;  
664 Josserand and Zaleski, 2003; Planchon and Mouche, 2010) where drop impacts are responsible for  
665 particle detachment and the creation of microtopography, which, in turns, creates pathways for  
666 runoff and further soil degradation processes. Nevertheless, avoidance strategies fed by real-time  
667 wind and precipitation data (collected at a 30 s time step) are powerful means to handle these  
668 issues, certainly to be included in the more general optimisation strategies suitable for the cultivated  
669 agrivoltaic plots.

670

671



672 **5. Conclusion**

673 Agrivoltaism represents a modern, relevant solution to the growing food and energy demands,  
674 associated with a global population increase, especially in the current climate change context. But  
675 still there are unresolved issues specific to the implementation of solar panels on the cultivated plots,  
676 for example regarding the adaptation of the plants to the forced intermittent shading conditions, or  
677 the impact of the panels on the hydrological budget and behavior of the plot. This paper has tackled  
678 the pending question of rain redistribution by "dynamic" solar panels, i.e. panels endowed with one  
679 degree of freedom in rotating around their supporting axis, so that their tilting angle may vary in time  
680 and be controlled on purpose, on a very short term of a few minutes.

681 A dramatic difference was observed and simulated, in terms of spatial patterns of rain redistribution  
682 on the ground, between the case of panels held flat and panels moved according to so-called  
683 "avoidance strategies" that consist in minimizing rain interception by the panels during the course of  
684 rain events (and eventually adapting the command of the panels to short-term changes in wind and  
685 rain conditions within a single event). The avoidance strategies resulted in far lesser coefficients of  
686 variation (i.e. heterogeneity measures) used to describe the spatial variations of the effective rain  
687 amounts falling on the ground, under the panels, between panels, or near the aplomb of the edges of  
688 the panels. The measures of heterogeneity obtained for avoidance strategies had low enough values  
689 to be compared with the fairly good uniformity scores used to quantify the ability of irrigation  
690 systems to deliver similar water amounts in the different zones of a given plot. Hence, it is likely that  
691 the most relevant irrigation strategies will suppress or attenuate the need for precision irrigation  
692 within the equipped plots. On the contrary, basic strategies that consist in holding the panels flat  
693 induce very strong spatial heterogeneities, with local effective rain amounts that exceed these of the  
694 control zone and may be responsible for increased runoff and erosion risks on bare soils, not to  
695 mention the risks associated with direct, repeated impacts on the plants that find themselves near  
696 the aplomb of the edge of the panels. The flat panel case has one additional disadvantage: the panels  
697 are never strictly flat, so that any transverse slope of comparable order will have the consequence of  
698 redirecting all the collected water towards a narrow outlet on the width of the panels.

699 However, the mechanistic AVrain model derived in this paper shows that the control exerted on the  
700 tilting angle of the panels is strong enough for the user to cope with most meteorological conditions



701 (rain intensity, wind direction and velocity) and realistic structure characteristics (height, length and  
702 spacing of the panels) to achieve the targeted short-term event-based optimisation of rain  
703 redistribution. It is very likely that more general and complex methods should be used when  
704 considering both the hydrological budget, crop growth and energy production, as well as seasonal  
705 objectives. To prepare ground, the soil part of the problem has also been investigated here, showing  
706 with Hydrus-2D simulations that rain redistribution patterns in soils resembled these observed on the  
707 soil surface, though less contrasted due to lateral diffusion processes on the soil surface (ponding) or  
708 within soils (at least where significant lateral dispersion coexists with gravity). Future research leads  
709 include a finer parameterization of Hydrus-2D for a stronger coupling with the results of the AVrain  
710 model, as a verification tool for the adaptation of simpler 1D approaches to model water budget,  
711 irrigation strategies and crop growth in agrivoltaic conditions (Khaledian et al., 2009; Mailhol et al.,  
712 2011; Cheviron et al., 2016) within global optimisation strategies.

713



714 **Code availability, data availability, sample availability**

715 Data collection and model development were performed in the frame of the Sun'Agri2B project that  
716 links the Sun'R SAS society with Irstea and other academic or non-academic partners. The copyright  
717 on all experimental and theoretical results presented here is governed by the consortium agreement  
718 of the Sun'Agri2B project.

719

720 **Appendices and supplementary links**

721 None

722

723 **Team list**

724 The first author is a PhD student, member of both the Sun'R SAS society and the "OPTIMISTE"  
725 research team of Irstea Montpellier, France, to which all co-authors also belong. OPTIMISTE stands  
726 for Optimization of the Piloting and Technologies of Irrigation, Minimization of InputS, Transfers in  
727 the Environment and is one of the research teams in the "G-Eau" joint research unit that addresses  
728 water management, actors and usages.

729

730 **Author contribution**

731 Yassin Elamri performed most of the experiments and developed the model, under the supervision of  
732 Bruno Cheviron and Gilles Belaud. Annabelle Mange contributed to the first stages of experiments  
733 and model development while Cyril Dejean and François Liron helped handling the metrological and  
734 technical parts of the work.

735

736 **Competing interests**

737 No known competing interests based on scientific grounds. However, there may be conflicts of  
738 interest on commercial grounds with societies other than Sun'R SAS also engaged in agrivoltaic  
739 activities.

740

741 **Disclaimer**

742 None

743

744 **Special issue statement**

745 None

746

747





748

749 **Acknowledgements**

750 This study was conducted within the frame of the SunAgri2b project, supported by Provence-Alpes-

751 Côte d'Azur and Rhône-Alpes Regions, CAPI, BPI France, Communauté de Communes Pays d'Aix,

752 Grand Lyon, the Agence Nationale pour la Recherche et la Technologie. The experimental platform

753 was co-funded by Irstea, Region Ile-de-France and Paris Entreprises.

754



755 **References**

- 756 ASAE. 1996. « Field evaluation of microirrigation systems ». *ASAE Standards. Amer. Soc. Agric. Engr.,*  
757 *St. Joseph, MI., n° EP405.1: 756-59.*
- 758 Barakat, M., B. Cheviron, B. Deweppe, C. Dejean, L. Lassabaterre, and R. Angulo-Jaramillo. 2016.  
759 « Numerical simulation of soil nitrate dynamics with Hydrus-2D for experimental maize plots  
760 under sprinkler and subsurface drip irrigation ». *Agricultural Water Management* 178:  
761 225-38.
- 762 Barnard, T., M. Agnaou, and J. Barbis. 2017. « Two Dimensional Modeling to Simulate Stormwater  
763 Flows at Photovoltaic Solar Energy Sites ». *Journal of Water Management Modeling.*
- 764 Best, A. C. 1950. « The Size Distribution of Raindrops ». *Quarterly Journal of the Royal Meteorological*  
765 *Society* 76 (327): 16-36.
- 766 Burt, C. M., A. J. Clemmens, T. S. Strelkoff, K. H. Solomon, R. D. Bliesner, L. A. Hardy, T. A. Howell, and  
767 D. E. Eisenhauer. 1997. « Irrigation Performance Measures: Efficiency and Uniformity ». *Journal of Irrigation and Drainage Engineering* 123 (6).  
768
- 769 Campolongo, F., J. Cariboni, and A. Saltelli. 2007. « An Effective Screening Design for Sensitivity  
770 Analysis of Large Models ». *Environmental Modelling & Software* 22 (10): 1509-18.
- 771 Cheviron, B., R. W. Vervoort, R. Albasha, R. Dairon, C. Le Priol, and J.C. Mailhol. 2016. « A Framework  
772 to Use Crop Models for Multi-Objective Constrained Optimization of Irrigation Strategies ». *Environmental Modelling & Software* 86: 145-57.  
773
- 774 Cook, L. M., and R. H. McCuen. 2013. « Hydrologic Response of Solar Farms ». *Journal of Hydrologic*  
775 *Engineering* 18 (5): 536-41.
- 776 Delahaye, J.-Y., L. Barthès, P. Golé, J. Lavergnat, and J.P. Vinson. 2006. « A Dual-Beam  
777 Spectropluviometer Concept ». *Journal of Hydrology* 328 (1-2): 110-20.
- 778 Diermanse, F.L.M. 1999. « Representation of Natural Heterogeneity in Rainfall-Runoff Models ». *Physics and Chemistry of the Earth, Part B: Hydrology, Oceans and Atmosphere* 24 (7):  
779 787-92.  
780
- 781 Dinesh, H., and J. M. Pearce. 2016. « The Potential of Agrivoltaic Systems ». *Renewable and*  
782 *Sustainable Energy Reviews* 54: 299-308.



- 783 Dupraz, C., H. Marrou, G. Talbot, L. Dufour, A. Nogier, and Y. Ferard. 2011. « Combining Solar  
784 Photovoltaic Panels and Food Crops for Optimising Land Use: Towards New Agrivoltaic  
785 Schemes ». *Renewable Energy* 36 (10): 2725-32.
- 786 Emmanuel, I., H. Andrieu, E. Leblois, N. Janey, and O. Payrastre. 2015. « Influence of Rainfall Spatial  
787 Variability on Rainfall? Runoff Modelling: Benefit of a Simulation Approach? » *Journal of*  
788 *Hydrology* 531: 337-48.
- 789 Lamm, F. R., and H. L. Manges. 2000. « PARTITIONING OF SPRINKLER IRRIGATION WATER BY A CORN  
790 CANOPY ». *Transactions of the ASAE* 43 (4): 909-18.
- 791 Faurès, J.-M., D.C. Goodrich, D. A. Woolhiser, and S. Sorooshian. 1995. « Impact of Small-Scale Spatial  
792 Rainfall Variability on Runoff Modeling ». *Journal of Hydrology* 173 (1-4): 309-26.
- 793 Gumiere, S. J., Y. Le Bissonnais, and D. Raclot. 2009. « Soil Resistance to Interrill Erosion: Model  
794 Parameterization and Sensitivity ». *CATENA* 77 (3): 274-84.
- 795 Gunn, R., and G. D. Kinzer. 1949. « The Terminal Velocity of Fall for Water Droplets in Stagnant Air ». *Journal of Meteorology* 6 (4): 243-48.
- 796
- 797 Harinarayana, T., and K. Sri Venkata Vasavi. 2014. « Solar Energy Generation Using Agriculture  
798 Cultivated Lands ». *Smart Grid and Renewable Energy* 05 (02): 31-42.
- 799 IPCC. 2011. *Renewable Energy Sources and Climate Change Mitigation: Summary for Policymakers*  
800 *and Technical Summary : Special Report of the Intergovernmental Panel on Climate Change.*  
801 New York: Cambridge University Press.
- 802 IPCC. 2014. *Climate Change 2014: Impacts, Adaptation and Vulnerability. Contribution of Working*  
803 *Group II to the Fifth Assessment Report of the Intergovernmental Panel on Climate Change.*  
804 New York: Cambridge University Press.
- 805 Jackson, N.A. 2000. « Measured and Modelled Rainfall Interception Loss from an Agroforestry System  
806 in Kenya ». *Agricultural and Forest Meteorology* 100 (4): 323-36.
- 807 Josserand, C., and S. Zaleski. 2003. « Droplet Splashing on a Thin Liquid Film ». *Physics of Fluids* 15 (6):  
808 1650.



- 809 Khaledian, M.R., J.C. Mailhol, P. Ruelle, and P. Rosique. 2009. « Adapting PILOTE model for water and  
810 yield management under direct seeding system: The case of corn and durum wheat in a  
811 Mediterranean context ». *Agricultural Water Management* 96 (5): 757-70.
- 812 Knapen, A., J. Poesen, G. Govers, G. Gysels, and J. Nachtergaele. 2007. « Resistance of Soils to  
813 Concentrated Flow Erosion: A Review ». *Earth-Science Reviews* 80 (1-2): 75-109.
- 814 Levia, D. F., and S. Germer. 2015. « A Review of Stemflow Generation Dynamics and Stemflow-  
815 Environment Interactions in Forests and Shrublands: STEMFLOW REVIEW ». *Reviews of*  
816 *Geophysics* 53 (3): 673-714.
- 817 Mailhol, J.C., P. Ruelle, S. Walser, N. Schütze, and C. Dejean. 2011. « Analysis of AET and yield  
818 predictions under surface and buried drip irrigation systems using the Crop Model PILOTE  
819 and Hydrus-2D ». *Agricultural Water Management* 98 (6): 1033-44.
- 820 Marrou, H. 2012. « Produire des aliments ou de l'énergie: faut-il vraiment choisir? - Evaluation  
821 agronomique du concept d'"agrovoltaïsme" ». Montpellier: Montpellier Sup'Agro.
- 822 Marrou, H., L. Dufour, and J. Wery. 2013a. « How Does a Shelter of Solar Panels Influence Water  
823 Flows in a Soil-crop System? » *European Journal of Agronomy* 50: 38-51.
- 824 Marrou, H., L. Guilioni, L. Dufour, C. Dupraz, and J. Wery. 2013b. « Microclimate under Agrivoltaic  
825 Systems: Is Crop Growth Rate Affected in the Partial Shade of Solar Panels? » *Agricultural*  
826 *and Forest Meteorology* 177: 117-32.
- 827 Marrou, H., J. Wery, L. Dufour, and C. Dupraz. 2013c. « Productivity and Radiation Use Efficiency of  
828 Lettuces Grown in the Partial Shade of Photovoltaic Panels ». *European Journal of Agronomy*  
829 44: 54-66.
- 830 Martello, M., N. Ferro, L. Bortolini, and F. Morari. 2015. « Effect of Incident Rainfall Redistribution by  
831 Maize Canopy on Soil Moisture at the Crop Row Scale ». *Water* 7 (5): 2254-71.
- 832 Morris, M. D. 1991. « Factorial Sampling Plans for Preliminary Computational Experiments ». *833*  
*Technometrics* 33 (2): 161.
- 834 Movellan, J. 2013. « Japan Next-Generation Farmers Cultivate Crops and Solar Energy ». *Renewable*  
835 *Energy World*. [http://www.renewableenergyworld.com/articles/2013/10/japan-next-](http://www.renewableenergyworld.com/articles/2013/10/japan-next-generation-farmers-cultivate-agriculture-and-solar-energy.html)  
836 [generation-farmers-cultivate-agriculture-and-solar-energy.html](http://www.renewableenergyworld.com/articles/2013/10/japan-next-generation-farmers-cultivate-agriculture-and-solar-energy.html).



- 837 Nearing, M. A., and J. M. Bradford. 1985. « Single Waterdrop Splash Detachment and Mechanical  
838 Properties of Soils<sup>1</sup> ». *Soil Science Society of America Journal* 49 (3): 547.
- 839 Niu, S., X. Jia, J. Sang, X. Liu, C. Lu, and Y. Liu. 2010. « Distributions of Raindrop Sizes and Fall  
840 Velocities in a Semiarid Plateau Climate: Convective versus Stratiform Rains ». *Journal of  
841 Applied Meteorology and Climatology* 49 (4): 632-45.
- 842 Osborne, M. 2016. « Fraunhofer ISE resurrects agrophotovoltaics ». *PVTECH*. [http://www.pv-  
843 tech.org/news/fraunhofer-ise-resurrects-agrophotovoltaics](http://www.pv-tech.org/news/fraunhofer-ise-resurrects-agrophotovoltaics).
- 844 Pereira, L. S., T. Oweis, and A. Zairi. 2002. « Irrigation Management under Water Scarcity ». *Agricultural Water Management* 57 (3): 175-206.  
845
- 846 Planchon, O., and E. Mouche. 2010. « A Physical Model for the Action of Raindrop Erosion on Soil  
847 Microtopography ». *Soil Science Society of America Journal* 74 (4): 1092.
- 848 Playán, E., and L. Mateos. 2006. « Modernization and Optimization of Irrigation Systems to Increase  
849 Water Productivity ». *Agricultural Water Management* 80 (1-3): 100-116.
- 850 Pujol, G., B. looss, and A. Janon. 2017. *Global Sensitivity Analysis of Model Outputs* (version 1.14.0).  
851 Package « sensitivity ».
- 852 Ravi, S., D. B. Lobell, and C. B. Field. 2014. « Tradeoffs and Synergies between Biofuel Production and  
853 Large Solar Infrastructure in Deserts ». *Environmental Science & Technology* 48 (5): 3021-30.
- 854 Simunek, J., M. Sejna, and M. Th. van Genuchten. 1999. « The HYDRUS-2D Software Package for  
855 Simulating the Two-Dimensional Movement of Water, Heat, and Multiple Solutes in  
856 Variably-Saturated Media (Version 2.0) ». Riverside, California: U.S. SALINITY LABORATORY,  
857 AGRICULTURAL RESEARCH SERVICE, U.S. DEPARTMENT OF AGRICULTURE.
- 858 Tang, Q., T. Oki, S. Kanae, and H. Hu. 2007. « The Influence of Precipitation Variability and Partial  
859 Irrigation within Grid Cells on a Hydrological Simulation ». *Journal of Hydrometeorology* 8 (3):  
860 499-512.
- 861 Te Chow, V. 1959. *Open Channel Hydraulics*. McGraw-Hill Book Company.
- 862 Van Hamme, T. 1992. « La pluie et le topoclimat ». *Hydrologie Continentale* 7 (1): 51-73.
- 863 Yuan, C., G. Gao, and B. Fu. 2017. « Comparisons of Stemflow and Its Bio-/Abiotic Influential Factors  
864 between Two Xerophytic Shrub Species ». *Hydrology and Earth System Sciences* 21 (3):  
865 1421-38.